Science of the Total Environment 843 (2022) 156841

Contents lists available at ScienceDirect

Science of the Total Environment

journal homepage: www.elsevier.com/locate/scitotenv

Nitrate removal by combining chemical and biostimulation approaches using micro-zero valent iron and lactic acid

Diana Puigserver, Jofre Herrero, José M. Carmona *

Department of Mineralogy, Petrology and Applied Geology, Faculty of Earth Sciences, University of Barcelona (UB), Water Research Institute (IdRA-UB), C/ Martí i Franquès, s/n, E-08028 Barcelona, Spain

HIGHLIGHTS

- A new nitrate removal method to solve issues raised by usual methods was developed.
- The use of ZVI as the sole reagent to remove nitrate produces the harmful ammonium.
- Ammonium is eliminated when ZVI combines with lactic acid causing the anammox process.
- Coupling ZVI and biostimulation of denitrifying flora effectively remove nitrate.

GRAPHICAL ABSTRACT

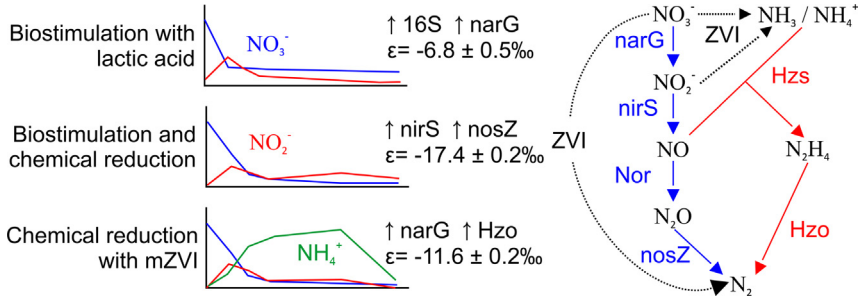

ARTICLE INFO

Editor: José Virgílio Cruz

Keywords:
Denitrification
Anammox
Gene
Enzyme
ZVI
Lactate

ABSTRACT

The occurrence of nitrate is the most significant type of pollution affecting groundwater globally, being a major contributor to the poor condition of water bodies. This pollution is related to livestock-agricultural and urban activities, and the nitrate presence in drinking water has a clear impact on human health. For example, it causes the blue child syndrome. Moreover, the high nitrate content in aquifers and surface waters significantly affects aquatic ecosystems since it is responsible for the eutrophication of surface water bodies. A treatability test was performed in the laboratory to study the decrease of nitrate in the capture zone of water supply wells. For this purpose, two boreholes were drilled from which groundwater and sediments were collected to conduct the test. The goal was to demonstrate that nitrate in groundwater can be decreased much more efficiently using combined abiotic and biotic methods with micro-zero valent iron and biostimulation with lactic acid, respectively, than when both strategies are used separately. The broader implications of this goal derive from the fact that the separate use of these reagents decreases the efficiency of nitrate removal. Thus, while nitrate is removed using micro-valent iron, high concentrations of harmful ammonium are also generated. Furthermore, biostimulation alone leads to overgrowth of other microorganisms that do not result in denitrification, therefore complete denitrification requires more time to occur. In contrast, the combined strategy couples abiotic denitrification of nitrate with biostimulation of microorganisms capable of biotically transforming the abiotically generated harmful ammonium. The treatability test shows that the remediation strategy combining in situ chemical reduction using micro-zero valent iron and biostimulation with lactic acid could be a viable strategy for the creation of a reactive zone around supply wells located in regions where groundwater and porewater in low permeability layers are affected by diffuse nitrate contamination.

1. Introduction

The presence of nitrogenous compounds (especially nitrate) is the most significant type of pollution affecting groundwater globally (Liu et al.,

* Corresponding author.
E-mail addresses: puigserverdiana@ub.edu (D. Puigserver), jofreherreroferran@ub.edu (J. Herrero), jmcarmona@ub.edu (J.M. Carmona).

http://dx.doi.org/10.1016/j.scitotenv.2022.156841
Received 10 March 2022; Received in revised form 7 June 2022; Accepted 16 June 2022
Available online 22 June 2022

2005; Serio et al., 2018; Canter, 2019) and is a major contributor to the poor condition of water bodies (Klement et al., 2017; Re et al., 2017). Moreover, the fact that this is pollution related to livestock-agricultural and urban activities (Dubrovsky and Hamilton, 2010; Ward et al., 2018) makes its presence in aquifers the cause of human and environmental impacts, at both spatial and temporal scales. The long exposure of subsurface materials to nitrate contamination accounts for the storage of a significant mass of nitrate in those materials (Ascott et al., 2016). This nitrate, which is difficult to remove, is dissolved in the porewater of layers of low hydraulic conductivity, into which it penetrated by molecular diffusion (Hinshaw et al., 2020). These layers will release nitrate to the environment by back-diffusion, even when the aquifers are cleaned or the more or less continuous supply of the nitrogenous compounds to the medium is interrupted as a result of changes in land use.

As is well known, there are multiple sources of nitrate, mainly of anthropogenic character (Shukla and Saxena, 2018). Among these sources, those related to the following can be distinguished: agricultural activities (Xue et al., 2012; Levy et al., 2017; Merchán et al., 2020), wastewater (Zhang et al., 2014; Wang et al., 2017), and urban activities (Paerl et al., 2016; Qin et al., 2019). Each of these sources can be identified by the isotopic composition ($\delta^{15}N$ and $\delta^{18}O$) of nitrate (Guo et al., 2021).

The presence of nitrate in drinking water has a clear impact on human health (Ward et al., 2018; Kaur et al., 2020) since it causes methemoglobinemia (blue child syndrome) (Wongsanit et al., 2015; Karunanidhi et al., 2021). Nitrate contamination has also been described to promote non-Hodgkins lymphoma (Wongsanit et al., 2015). In addition, the relationship between colon and gastrointestinal cancer with repeated consumption of nitrate-rich waters has been increasingly studied (Peng et al., 2016; Schullehner et al., 2018; Temkin et al., 2019). Moreover, the high content of this contaminant in the aquatic environment, especially in aquifers (Hansen et al., 2016; Di Lorenzo et al., 2021) and surface water bodies (Bhateria and Jain, 2016; Lasagna et al., 2016), has a marked impact on aquatic ecosystems (Chang et al., 2015) since it is responsible for the eutrophication of surface water bodies (Kopprio et al., 2014; Romanelli et al., 2020) and is very often the cause of high mortality of fish and other organisms (Demeke and Tassew, 2016).

Natural denitrification of nitrogen species occurs in the hydrogeological environment (Rivett et al., 2008; Park et al., 2016; Shukla and Saxena, 2018; Biddau et al., 2019). Biotic denitrification has been described as a dissimilatory reduction reaction of nitrate (NO_3^-) to nitrogen gas (N_2). The total mineralization of this compound takes place through a chain of reactions in which progressively more reduced nitrogen is present so that NO_3^- is sequentially converted to nitrite (NO_2^-), nitric oxide (NO), nitrous oxide (N_2O), and, finally, harmless N_2, as shown in the Reaction 1 sequence (Della Rocca et al., 2007). The NO_3^- to NO_2^- reaction of this sequence can be carried out by a phylogenetically diverse group of bacteria. Some of the enzymes (e.g., narG and napA) responsible for this process have been identified (Wallenstein et al., 2006). In contrast, the three later reactions are limited to a smaller number of bacteria and metabolic pathways. Specifically, they are limited to the following reductases: NO_2^- reductases (nirS and nirS), nitric oxide reductase (Nor), and nitrous oxide reductase (nosZ) (Braker et al., 2000; Huang et al., 2011).

$$NO_3^- \rightarrow NO_2^- \rightarrow NO \rightarrow N_2O \rightarrow N_2 \text{ Reactions 1 sequence}$$

Microbial nitrate reduction is coupled to the anaerobic oxidation of an organic substrate, and use NO_3^- or NO_2^- as a terminal electron acceptor (mediated by heterotrophic bacteria) (Rivett et al., 2008; Capodaglio et al., 2016). Heterotrophic denitrification, on which most denitrification-based treatments are based, can be described by the general Reaction 2 sequence (Jørgensen et al., 2004), as follows:

$$5CH_2O + 4NO_3^- \rightarrow 2\,N_2 + 4HCO_3^- + CO_2 + 3\,H_2O \text{ Reaction 2 sequence}$$

where CH_2O represents a generic organic compound.

The low bioavailability of organic carbon in subsurface materials has been identified as one of the major limiting factors for denitrification (Sunger and Bose, 2009; Jahangir et al., 2012). The supply of an external organic substrate to the aquifer can compensate for this deficit and can easily favor the bacterial growth of denitrifying microorganisms (Qambrani et al., 2013; Zhang et al., 2018).

Autotrophic denitrification (Molognoni et al., 2017) consists of the reduction of NO_3^- in the presence of Fe^{2+} or S^{2-}, S^{1-}, or S^0 by a biotic or abiotic process. The Reaction 3 group describing this type of process includes the following:

$$8Fe^{2+} + NO_3^- + 13H_2O \rightarrow 8FeOOH + NH_4^+ + 14H^+ \text{ Reaction 3 group} \quad (1)$$

$$8Fe^{2+} + 2NO_3^- + 11H_2O \rightarrow 8FeOOH + N_2O + 14H^+ \text{ Reaction 3 group} \quad (2)$$

$$10Fe^{2+} + 2NO_3^- + 14H_2O \rightarrow 10FeOOH + N_2 + 18H^+ \text{ Reaction 3 group} \quad (3)$$

$$2Fe^{2+} + NO_3^- + 3H_2O \rightarrow 2FeOOH + NO_2^- + 4H^+ \text{ Reaction 3 group} \quad (4)$$

$$12Fe^{2+} + NO_3^- + 13H_2O \rightarrow 4Fe_3O_4 + NH_4^+ + 22H^+ \text{ Reaction 3 group} \quad (5)$$

$$12Fe^{2+} + 2NO_3^- + 11H_2O \rightarrow 4Fe_3O_4 + N_2O + 22H^+ \text{ Reaction 3 group} \quad (6)$$

$$15Fe^{2+} + NO_3^- + 13H_2O \rightarrow 5Fe_3O_4 + N_2 + 28H^+ \text{ Reaction 3 group} \quad (7)$$

$$12Fe^{2+} + 2NO_3^- + 13H_2O \rightarrow 4Fe_3O_4 + NH_4^+ + 22H^+ \text{ Reaction 3 group} \quad (8)$$

$$5FeS_2 + 14NO_3^- + 4H^+ \rightarrow 7\,N_2 + 10SO_4^{2-} + 5Fe^{2+} + 2H_2O \text{ Reaction 3 group} \quad (9)$$

Another process leading to the decrease in nitrogen species in the aquifer environment is anaerobic ammonium oxidation (anammox). Reaction 4 describes this process (Langone et al., 2014; Smith et al., 2015; Caschetto, 2017; Lee et al., 2021), as follows:

$$NH_4^+ + 1.32NO_2^- + 0.066HCO_3^- + 0.13H^+ \leftrightarrow 1.02N_2 + 0.26NO_3^- + 0.066CH_2O + 0.5\,N_{0.15} + 2.03H_2O \text{ Reaction 4}$$

This process gives rise to the oxidation of ammonium (which acts as an electron donor) and the reduction of NO_2^- (which acts as an electron acceptor) under anoxic conditions, resulting in the formation of N_2 gas and, to a lesser extent, nitrate (Jetten et al., 2001; Miao et al., 2019). This process is mediated, among others, by nitrite reductase (nirS) and hydrazine synthase (Hzs) enzymes (Zhou et al., 2017).

The monitoring of these processes is key and is often carried out by integrating chemical and isotopic techniques, as well as molecular techniques (Kim et al., 2015; Park et al., 2016; Biddau et al., 2019).

The more or less continuous supply of nitrogenous species to the environment and/or the presence of a large mass of these species in different hydrogeological contexts requires the implementation of methods for minimizing these compounds. Traditionally, the most commonly used in situ techniques have been those related to the biostimulation of indigenous bacterial flora through the addition of an organic substrate, such as methanol, ethanol, acetate, and lactate, which acts as an electron donor and as a carbon source for these microorganisms (Park et al., 2014; Sheng et al., 2018). Bioaugmentation, as in situ bioremediation technique, has been used less frequently, given the large amount of denitrifying microorganisms in the medium (Ruan et al., 2020).

Although bioremediation techniques are among the most widely used, they present numerous problems. Among which is the fact that microbial overgrowth can occur, causing biologging (McLeod et al., 2018; Mohanadhas and Kumar, 2019; Zhang et al., 2020), which results in the following: i) reduced hydraulic conductivity of the aquifer (Zhong and Wu, 2013) and ii) decreased efficiency of the injection and extraction

wells of bioremediation systems. Another problem is that bacterial competition for available electrons is promoted, which often involves the displacement of the microbial communities of most interest for the biogeochemical process to be promoted (Bertrand et al., 2015).

Although, to a lesser extent, chemical nitrate reduction treatments by addition to the medium of Fe^0 (metallic iron) in the form of micrometric-sized particles (micro-zero valent iron [mZVI]) have also been described (Liu and Wang, 2019). In this case, these are mainly abiotic reactions, including the Reaction 5 group (Chen et al., 2005; Rodríguez-Maroto et al., 2009), as follows:

$$Fe^0 \rightarrow Fe^{2+} + 2e^- \text{ Reaction 5 group} \quad (1)$$

$$5Fe^0 + 2NO_3^- + 12H^+ \rightarrow 5Fe^{2+} + N_2 + 6H_2O \text{ Reaction 5 group} \quad (2)$$

$$4Fe^0 + 2NO_3^- + 10H^+ \rightarrow 4Fe^{2+} + NH_4^+ + 3H_2O \text{ Reaction 5 group} \quad (3)$$

$$Fe^0 + 2NO_3^- + 4H^+ \rightarrow Fe^{2+} + 2NO_2^- + 2H_2O \text{ Reaction 5 group} \quad (4)$$

$$6Fe^{2+} + NO_2^- + 8H^+ \rightarrow 6Fe^{3+} + NH_4^+ + 2H_2O \text{ Reaction 5 group} \quad (5)$$

Under acidic conditions:

$$Fe^0 + 2H^+ \rightarrow Fe^{2+} + H_2 \text{ Reaction 5 group} \quad (6)$$

Under neutral conditions:

$$Fe^{2+} + Fe^{3+} + H_2O \rightarrow \text{iron oxides} + H^+ \text{ Reaction 5 group} \quad (7)$$

$$Fe^0 + 2H_2O \rightarrow \text{iron oxides} + H^+ \text{ Reaction 5 group} \quad (8)$$

Among the above reactions, it is noteworthy, on the one hand, that when Fe^0 oxidizes it produces H_2 gas, which is one of the most important electron donors in the medium. These electrons can be used by the microorganisms, which favor autotrophic denitrification (Liu et al., 2018). However, on the other hand, some of the nitrate degradation reactions in the presence of Fe^0, e.g., Reaction 5 (3), result in the formation of ammonium, which is toxic at high concentrations (Di Lorenzo et al., 2015).

The use of combined in situ chemical reduction (ISCR) and biostimulation methods in aquifers contaminated by nitrogen species is not a frequent practice. However, this combination of methods has shown satisfactory results in the treatment of other types of contamination, such as those shown by Herrero et al. (2019) in chloroethenes.

The working hypothesis of the current study is that, in regional diffuse contamination, nitrate concentration in groundwater can be decreased using combined methods with mZVI and biostimulation with lactic acid. To demonstrate this hypothesis, a treatability test was performed in the laboratory with microcosm experiments to study the decrease in the nitrate concentration of groundwater in the capture zone of a water supply well. It is intended that the laboratory test results could be used to analyze combined in situ remediation strategies in future field-scale implementation. These strategies would consist of the creation of reactive zones around groundwater supply wells. This would minimize the treatment costs of nitrate-contaminated groundwater before it is extracted by these wells.

The following specific objectives were set for studying the decrease in nitrates in the above-mentioned capture zone: (1) analysis of denitrification rates for the different remediation methods tested, based on chemical, isotopic, and molecular techniques; (2) establishment of the sequence of hydrogeochemical and biogeochemical processes occurring according to the different scenarios created; and (3) assessment of the efficiency of nitrate mobilization depending on the remediation method tested to establish the most suitable strategy.

A field zone was chosen the municipality of Torrefeta and Florejacs (La Segarra shire), to obtain sediment and groundwater from the capture zone of a well for the supply of drinking water to carry out the treatability test. This municipality is located in the nitrate pollution vulnerable zone #6 of Catalonia (Spain, Fig. 1A). This shire was declared a vulnerable zone for nitrate contamination from agricultural sources by Decree 283/1998 of October 21, 1998.

2. Site description

The monitoring network of the Catalan Water Agency (CWA) in this vulnerable zone is formed by two municipal supply wells for the village (W1 and W2, Fig. 1B). In fact, well W1 is formed by two wells, 3.7 and 7 m deep (both with a diameter of 1.5 m) and is connected by a 3 m gallery. Both wells are located in Tertiary (Oligocene) and Quaternary (Pleistocene and Holocene) materials of the Central Catalan Depression (Fig. 1B). The lower Oligocene materials (Fig. 1B) consist mainly of red clays and gray marls with interbedded sandstones and limestones. The Quaternary

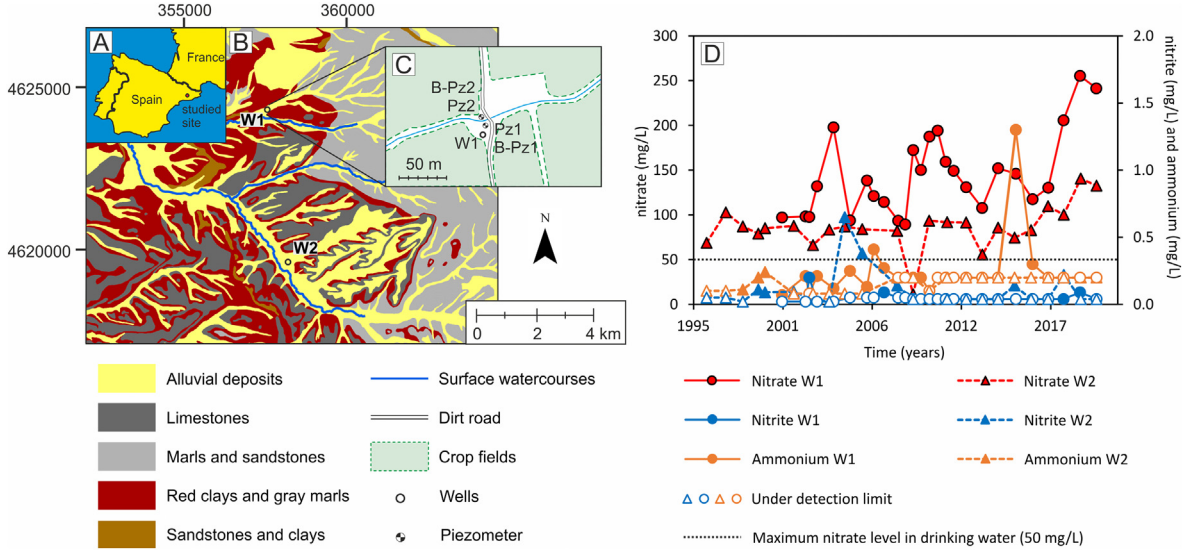

Fig. 1. (A) Geographical situation of the site where sediments and groundwater were collected for the treatability test. (B) Geological context of the site and location of the supply wells W1 and W2 that form part of the control network of the CWA. Coordinates in the UTM system (Universal Transverse Mercator coordinate system (meters). (C) Detail of the geographical location of the boreholes B-Pz1 and B-Pz2. Supply well W1 is also shown. (D) Temporal evolution of nitrate, nitrite and ammonium in the groundwater of the two wells (W1 and W2) of the CWA monitoring network.

materials are alluvial deposits of the Sió River, which correspond to ochre and brown sandy silts containing gravels and limestone pebbles and some sandstones. They are subangular or subrounded pebbles with little internal organization that constitute approximately 30 % of these alluvial materials. Tertiary and Quaternary materials constitute aquifer formations.

Sediment for the treatability test was obtained from two research boreholes (B-Pz2 and B-Pz1, Fig. 1C). See detailed lithostratigraphic description of these boreholes in Figs. SM-1 and SM-2 in the Supplementary material (SM) document. These boreholes were drilled for the construction of two conventional observation piezometers (Pz2 and Pz1 in Fig. 1C), which were screened between a depth of 4 and 6 m in both cases. Groundwater for the test was pumped from these piezometers. The boreholes were drilled 10 m away from the mentioned supply well (W1) (Fig. 1C) and within its capture zone. At the local scale, the geological testing conducted in the two research boreholes (B-Pz1 and B-Pz2, Fig. 1C) showed that the Quaternary alluvial aquifer was unconfined. The boreholes reached the bottom materials of the unconfined aquifer. These materials consisted of marls and marlstones of very low hydraulic conductivity (from 1.0E-06 to 1.0E-05 cm/s). Below the marlstones is the Tertiary aquifer, which is confined.

The mentioned nitrate pollution vulnerable zone #6, where sediments and groundwater for the treatability test were taken, has been characterized by a significant increase in nitrate concentration over the years. In particular, in supply well W1 (Fig. 1C), nitrate concentrations remain above 100 mg/L (Fig. 1D), and in recent years a trend of sustained growth in the minimum values recorded has been observed, along with occasional increases in ammonium.

3. Materials and methods

3.1. Design, setup, and dimensioning of the microcosm-type treatability test with combined remediation methods

The treatability test consisted of four microcosm experiments in which the following scenarios were simulated (Table 1): i) natural attenuation (NAT), ii) biostimulation of the microbial flora with the addition of lactate (BLA, in the form of lactic acid) as the major carbon source and electron donor, iii) ISCR abiotic degradation with the addition of mZVI (ZVI), and iv) simulation of a biostimulation strategy with lactic acid combined (COMB) with ISCR using mZVI.

Each microcosm experiment was performed in duplicate; therefore, there were two actives and two controls per experiment (i.e., four bottles for each experiment). In the actives, microbial activity was present, while in the controls microorganisms were killed.

Table 1
Treatability test through microcosm experiments performed to asses and dimension the maximum efficiency in decreasing nitrate concentration to create a reactive zone around supply wells in their capture zones.

Microcosm experiment	Treatment performed	Bottles (duplicates are included)
		Active (A)/Control (C)
#1	Natural attenuation (NAT)	A-NAT 1
		A-NAT 2
		C-NAT 1
		C-NAT 2
#2	Biostimulation with lactate as electron donor using lactic acid (BLA)	A-BLA 1
		A-BLA 2
		C-BLA 1
		C-BLA 2
#3	ISCR with Fe^0 microparticulate (ZVI)	A-ZVI 1
		A-ZVI 2
		C-ZVI 1
		C-ZVI 2
#4	Combination of biostimulation and mZVI (COMB)	A-COMB 1
		A-COMB 2
		C-COMB 1
		C-COMB 2

The bacterial activity of the control experiments was eliminated by sterilization of the sediment and groundwater used in an autoclave (model Autester 75 E DRY-PV; Selecta, Barcelona, Spain), in a similar way as that described by Puigserver et al. (2016a,b). Additionally, and in accordance with Trevors (1996), 50 mL of a 147 mM $HgCl_2$ stock solution (mercury II chloride, puriss. p.a.; Riedel-Deha, Seelze, Germany) was added as a bactericide to each control experiment. Microcosm experiments were carried out in 2 L Pyrex glass bottles. Each of the bottles contained 1 kg of sediment from the aquifer and 1.5 L of groundwater (characterized by an electrical conductivity of 1761 μS/cm, pH of 7.29, Eh of 77 mV, and a dissolved oxygen concentration of 3.08 mg/L).

The two research boreholes B-Pz1 and B-Pz2 (Fig. 1C) were drilled using the rotation technique with a diamond drill bit, and a continuous core of sediment was obtained according to Puigserver et al. (2013, 2016a,b) for testing and for experiments.

The boreholes were subsequently equipped as conventional piezometers and screened between a depth of 4 and 6 m, from where the aquifer water used for the treatability test was pumped and collected.

As for the reagents used, 10 mg of food-grade mZVI (Carus®) was introduced into the bottles at the start of experiments #3 and 4 (Table 1), and a total of 10 mL of food-grade lactic acid (98 %, Vadequimica-Barcelona) was used throughout the treatability test in experiments #2 and #4.

Once the sediment, water, and reagents were introduced, the experiment bottles were equipped with Minivert® valves and properly sealed with insulating tape to periodically sample the water inside.

Methanol (MeOH; ISO Pro Analysis; Merck, Darmstadt, Germany) was used to clean and sterilize the remaining used materials during preparation of the bottles.

Experiments were conducted in a flexible vinyl anaerobic chamber (Globe box Coy Laboratory Products, Grass Lake, MI, USA).

3.2. Water sampling protocols in the bottles of the experiments. Conservation procedures. Sample pretreatments. Parameters determined

To conduct the treatability test, once the bottles of the microcosm experiments were prepared, they were placed in the anaerobic chamber, where the water of the bottles was periodically monitored. An integration of chemical, isotopic, and molecular analyses was performed. Table 2 shows the samples taken during the treatability test.

The sampling protocols followed during the monitoring of water in the bottles of the microcosm experiments consisted of extracting a specific volume of water (Table 2) using syringes and opening the Minivert® valve of the bottle to be monitored.

Further information on chemical and isotopic analyses and molecular determinations conducted in microcosm water samples can be found in the SM document. This document also includes detailed information on analytical techniques to perform chemical and isotopic analyses and methodologies for molecular determinations.

3.3. Data processing

3.3.1. Processing of chemical and isotopic analytical data

The interpretation of the treatability test was performed by integrating the evolution in the microcosm experiments of the concentrations of nitrogen compounds. This integration was carried out with respect to the redox conditions characterized from the analysis of the redox sensitive species, similarly to what was done by Munz et al. (2019). In addition, the isotopic fractionation of the ^{15}N of nitrate was studied, similarly to that performed by Vavilin and Rytov (2015), which allowed for characterization of the enrichment factor (Ɛ) produced by the biotic denitrification process (Wells et al., 2019) and abiotic reduction of nitrate produced by the addition of mZVI (Grau-Martínez et al., 2019) as the main mechanisms of nitrate mobilization. Subsequently, all of these results obtained were interpreted in the framework of the molecular determinations (see Section 3.3.2).

Table 2
Samples taken during the microcosm experiments and volumes of water extracted for each parameter or group of parameters.

Time		Experiments	Volume of water extracted (mL)			
(Min)	(Days)		Anions	NH_4^+, Fe^{2+}, Mn^{2+}	$\delta^{14}N$ (nitrate)	Microorganisms
0	0	NAT, BLA, ZVI and COMB	1	20	140	20
1440	1	NAT, BLA, ZVI and COMB	1	20	140	Not collected
2880	2	NAT, BLA, ZVI and COMB	1	20	140	Not collected
4320	3	NAT, BLA, ZVI and COMB	1	20	140	20
10,080	7	NAT, BLA, ZVI and COMB	1	20	140	20
14,400	10	NAT, BLA, ZVI and COMB	1	20	140	20

3.3.2. Processing of data from molecular determinations

Once the analyzed genes were identified, the software of the equipment was used to determine the threshold cycle (Ct) value (which is the cycle in which the DNA concentration exceeds the established threshold). Specifically, the threshold values were 0.0224 for the nirS, nirS, and nosZ primers; 0.0143 for the narG and 16S (1055f-1392r) primers; and 0.0172 for the 16S (341f-785r) and Hzo primers. No presence was detected in the HzsA, HzsB and nor primer sets. In all cases, the average and standard deviation of the data were calculated (in semiquantitative units of cycles where the threshold value was reached).

For interpretation, values from the same set of primers are related to each other since all samples were analyzed together and under the same conditions (however, it is not possible to compare different sets of primers). In addition, an increase in the Ct value indicates that there is a lower concentration of microorganisms, so that the concentration of DNA (or microorganisms) is inversely proportional to the Ct.

4. Results and discussion

4.1. Evolution of the concentrations and isotopic composition of nitrogen compounds in the microcosm experiments

4.1.1. Natural attenuation

The evolution of nitrate concentrations in the active NAT experiment (Fig. 2A, NAT) shows how the indigenous microbial communities have high nitrate degradation capacity under natural conditions (Park et al., 2016) since after 3 days (4320 min) the nitrate concentration decreased by 81.76 %, with a value below the parametric limit of 50 mg/L established by European Union legislation for drinking water (European Union Directive, 2020), above which human health is at risk. The degradation rate throughout the NAT experiment was 0.23 day^{-1} or 0.02 h^{-1}. This degradation rate, although below the value of 0.2 h^{-1} reported by Ghane et al. (2015), shows that denitrification did indeed take place under conditions of natural attenuation. The decrease in nitrate concentrations was accompanied by a maximum concentration of nitrite of 4 mg/L after 1 day (1440 min), which is consistent with the fact that denitrification is often favored by the complete mineralization of the initial nitrate to N_2 gas (Tiedje, 1994; Istok et al., 2007; Keiner et al., 2015).

The mentioned degradation rate of nitrate in the active NAT experiment was also demonstrated by comparing the nitrate percentage mobilization between active and control experiments. In the former, the value was of 95.33 % at the end of the experiment, while in the latter it was only 13.95 %, similar to what Ashok and Hait (2015) described.

In the NAT experiment, denitrification produced isotopic fractionation in nitrate (with an increase in $\delta^{15}N$), mainly in the active experiments (Fig. 3). Considering that experiments were conducted in duplicate, on day 0 (0 min, start of the treatability test) the $\delta^{15}N$ nitrate value was 4.06 ‰ (Fig. 3), with practically no value dispersion. In contrast, on day 10 (14,400 min, when experiments finished) the range of $\delta^{15}N$ values varied between 16.2 ‰ and 25.0 ‰. This range of values resulted in denitrification between the first and final day, leading to a range of $\Delta\delta^{15}N$ values in nitrate that varied between 12.1 ‰ and 20.09 ‰, respectively, with a mean value of 16.1 ‰. With the same $\delta^{15}N$ values between day 0 (0 min) and day 10 (14,400 min), the resulting Ɛ factor was -5.2 ± 0.3 ‰, which is in the range of isotopic enrichment factors between -5 and -30 ‰ of groundwater described by Aravena and Robertson (1998) and Wenk et al. (2014), among others.

4.1.2. Lactic acid biostimulation

The biostimulation experiment with lactic acid (Fig. 2C, BLA), as an electron donor in the form of lactate ion, generated overgrowth of the set of microbial consortia present in groundwater and sediment (see, for example, Fig. 4A in Section 4.3), similar to what was observed by Puigserver et al. (2016a,b), which generated a decrease in the efficiency of nitrate degradation. This implies that the nitrate concentrations did not fall below the parametric value of 50 mg/L until 7 days (10,080 min) after the experiment was initiated (Fig. 2C), which was accompanied by a high accumulation of nitrite (with maximum values of 5 to 6 mg/L), similar to what was observed by Chen et al. (2012).

The different degree of development of bacterial communities (see Fig. 4 in Section 4.3) was also revealed by a large dispersion of degradation rates ranging from 0.25 to 0.39 $days^{-1}$, which showed that there was heterogeneity in the distribution of the microbial flora, especially that living in the sediment (Pedersen et al., 2015). This was also observed in the different percentages of decreases in nitrate, with values in the active experiment ranging from 94.43 to 98.26 %, whereas in the controls the mobilization percentage was much lower, with an average value of 18 % and with little dispersion.

The $\delta^{15}N$ values in the BLA experiment were higher than those recorded in the case of the NAT experiment (Fig. 3). Thus, in the BLA experiment, $\Delta\delta^{15}N$ values ranging from 22.07 to 25.26 ‰, with a mean value of 23.67 ‰, were observed. With the same $\delta^{15}N$ values between day 0 (0 min) and day 10 (14,400), the resulting Ɛ factor was -6.8 ± 0.5 ‰. Although biostimulation allows the microbial activity to favor nitrate degradation, the existence of bacterial competition for electrons supplied by lactate leads to a loss of efficiency in the total mineralization of nitrate.

4.1.3. Chemical reduction with micro-zero valent iron

The evolution of nitrate concentrations in the ZVI experiment, with mZVI as a reducing agent (Fig. 2E, ZVI), showed a higher degradation rate (varying between 0.42 and 0.32 $days^{-1}$, with a mean value of 0.38 $days^{-1}$) than in the case of the BLA experiment. This is attributable to the fact that the use of mZVI partially inhibited the activity of denitrifying microorganisms (Xie et al., 2017), especially immediately after mZVI was placed with the sediment in the bottles of this experiment on day 0 (0 min). However, the progressive consumption of mZVI promoted the recovery of microbial activity (Cullen et al., 2011). In contrast to the NAT and BLA experiments, the control experiment showed a higher nitrate degradation rate because of the abiotic degradation caused by the reduction promoted by mZVI (Y. Zhang et al., 2019).

According to Reaction 5 (3), the degradation of nitrate in the presence of mZVI as a reducing agent was accompanied by an increase in ammonium concentration, as observed by Jia et al. (2017), Yang et al. (2018), Liu and Wang (2019), and Su et al. (2020). This was observed in both active

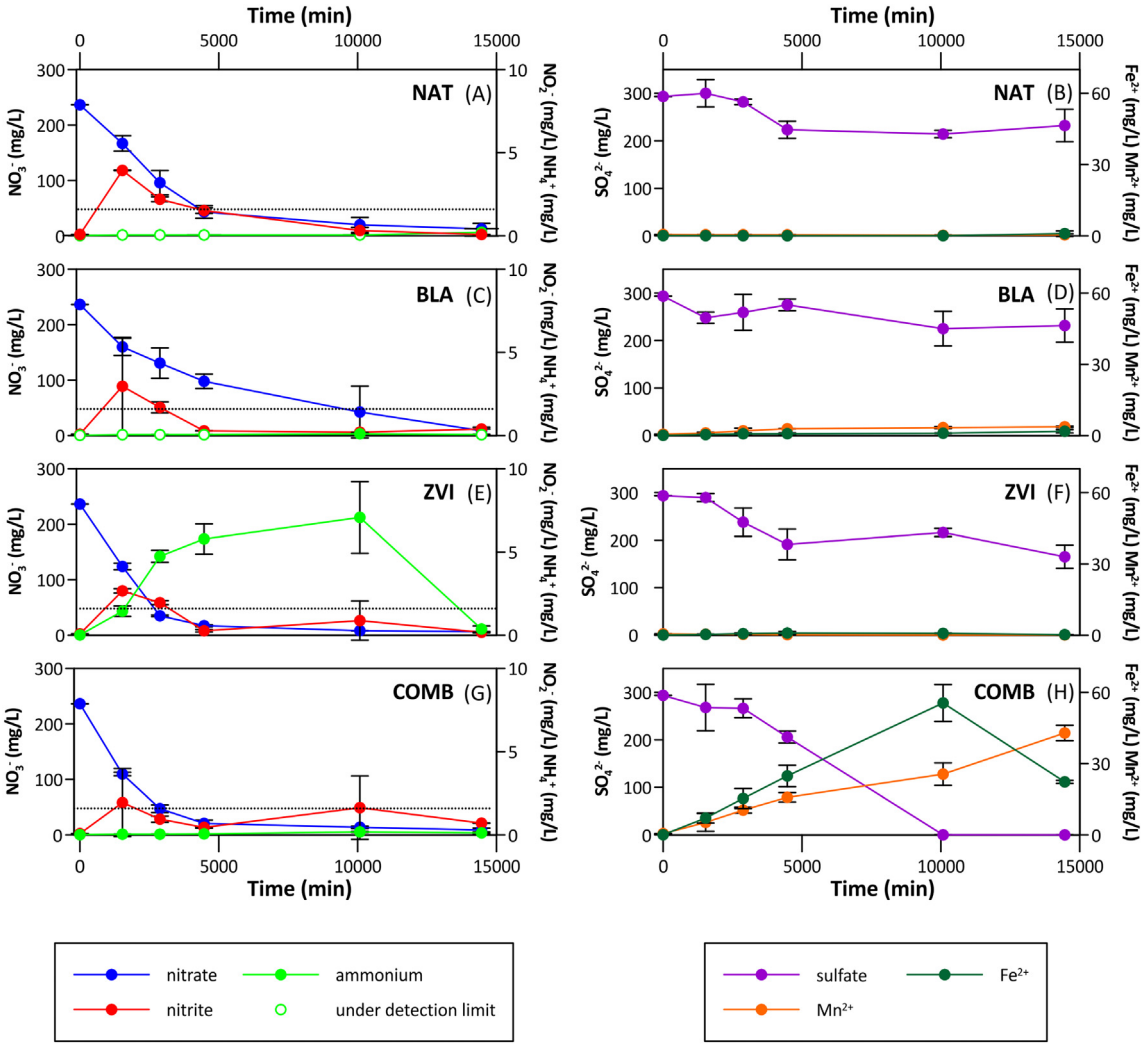

Fig. 2. Temporal evolution of concentrations of nitrogen species and other redox-sensitive species in the active microcosm experiments. The average values (±the standard deviation) are plotted. Left plots (A, C, E, G): nitrate, nitrite, and ammonium. Right plots (B, D, F, H): sulfate, Fe^{2+} and Mn^{2+}. Natural attenuation (NAT), Biostimulation with lactic acid (BLA), Chemical reduction with mZVI (ZVI), Combined chemical reduction and biostimulation (COMB). The horizontal dotted line on the nitrate evolution plots marks the parametric limit of 50 mg/L established for drinking water, above which human health is at risk.

(Fig. 2E, ZVI) and control experiments. It is noteworthy that in the two actives (duplicates) ammonium production was lower than in the two controls, which suggests that there are microorganisms capable of degrading ammonium. In contrast, the nitrite concentrations recorded in the active experiments (with maximum values up to 2.6 mg/L) were lower than those recorded in the NAT and BLA experiments.

The isotopic evolution of $\delta^{15}N$ of nitrate (Fig. 3) showed a higher isotopic fractionation in the ZVI experiment than in the NAT experiment. Thus, in the active ZVI experiments, the nitrate $\Delta\delta^{15}N$ value varied between 40.7 and 44.6 ‰, which represents a mean value of 42.7 ‰ and is about 20 units more than in the NAT experiment. This higher isotopic fractionation was also evidenced by a greater ^{15}N nitrate Ɛ factor, which was -11.6 ± 0.2 ‰, below that reported by Grau-Martínez et al. (2019), who recorded a value of -29.5 ± 2.7 ‰.

4.1.4. Combination of mZVI and biostimulation

The evolution of nitrate concentrations in the COMB experiment, with the combined strategy of mZVI and biostimulation with lactic acid (Fig. 2G, COMB), showed an evolution quite similar to that in the ZVI experiment (Fig. 2E, ZVI). Thus, nitrate concentrations were below 50 mg/L 2 days (2880 min) after the start of the experiment. However, the biostimulation of bacterial communities in the COMB experiment (Fig. 2C) slightly decreased the nitrate degradation rate (ranging from 0.27 to 0.34 $days^{-1}$), similar to what was observed in the experiment exclusively with biostimulation (Fig. 2C, BLA). Nevertheless, in counterpart, no remarkable ammonium production was observed in the COMB experiment (Fig. 2G, COMB), as was the case in the ZVI experiment (Fig. 2E, ZVI). This confirms the greater efficiency of combining the use of mZVI with biostimulation in reducing toxicity since the decrease in nitrate is accompanied by little formation of toxic ammonium. Due to the absence of microbial activity in the control experiments, the controls of the COMB experiment showed a similar evolution of nitrate concentrations to those of the ZVI controls.

Isotopic fractionation was also recorded in the COMB experiment (Fig. 3), with $\Delta\delta^{15}N$ values higher than those in the other experiments. Thus, $\Delta\delta^{15}N$ values varied in the COMB experiment between 54.3 and 64.3 ‰, with a mean value of 59.4 ‰, which, specifically compared to the ZVI experiment, were higher than in this experiment. This agrees with the mentioned higher degradation efficiency because of the combination of biotic and abiotic degradation. Furthermore, although in the COMB experiment, the degradation of nitrate to nitrite (or ammonium) followed the same pathway as in the case of the ZVI experiment. In the COMB experiment, the Ɛ factor was higher (-17.4 ± 0.2 ‰) than in the ZVI experiment. Fig. 3 also shows that a large part of the isotopic fractionation in the COMB experiment was caused by the abiotic nitrate degradation reaction caused by the presence of mZVI in that experiment.

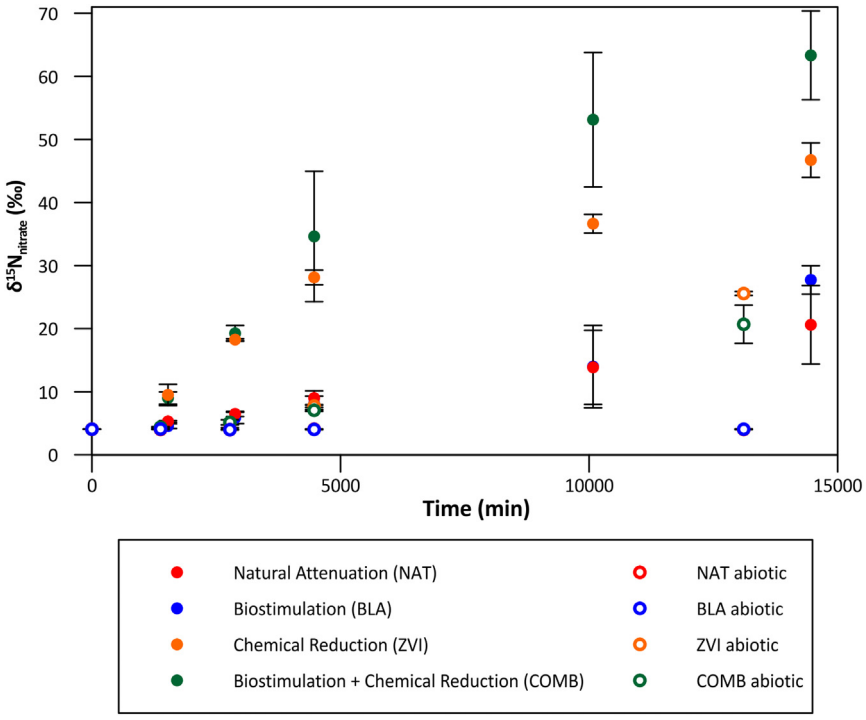

Fig. 3. Evolution of nitrate $\delta^{15}N$ isotopic composition in the different experiments. The average values (±the standard deviation) are plotted. Abiotic experiments are the control experiments.

4.2. Evolution of redox-sensitive species

In general, an increase in Mn^{2+} concentrations was observed in the BLA and COMB experiments (Figs. 2D, H), up to 2.5 and 40.5 mg/L, respectively, which confirms that Mn reduction occurred (Trouwborst et al., 2006; McMahon et al., 2018).

In the case of Fe^{2+} concentrations, small increases were detected in the NAT and BLA experiments (Fig. 2B, D), up to 2 and 2.5 mg/L, respectively, and high increases in the COMB experiment (Fig. 2H) up to 60 mg/L were observed. This reveals that in the NAT and BLA experiments Fe-reducing conditions were reached, which is in agreement with Abiriga et al. (2021), and more reducing conditions were found in the case of COMB.

The evolution of sulfate concentrations showed that in the NAT experiment there was a decrease of 30 % of the initial concentration after 3 days (4320 min), which remained constant thereafter (Fig. 2B, NAT). In the BLA experiment, sulfate concentrations did not significantly decrease until 7 days (10,080 min, Fig. 2D, BLA).

In the ZVI experiment, sulfate decreases were slightly higher than those recorded in the NAT experiment—about 43 % after 3 days (4320 min)—but, unlike in the NAT experiment, concentrations continued to decrease up to 50 % at the end of the experiment on day 10 (14,400 min, Fig. 2F, ZVI). The decrease in sulfate was accompanied by low Fe^{2+} concentrations (that did not reach 1 mg/L throughout the experiment; Fig. 2F, ZVI). This reveals the precipitation of iron sulfide as a result of sulfate reduction (Christensen et al., 2000; Karimian et al., 2018).

In the case of the COMB experiment (Fig. 2H, COMB), sulfate concentrations were below the detection limit after 7 days (10,080 min), implying that 100 % was eliminated because of highly reducing conditions, possibly even methanogenic.

4.3. Evolution of genes characteristic of denitrification and anammox processes

The analysis of the evolution of the microbial communities detected with the 16S primers (1055f-1392r, in Table 1 in the SM document) showed that the highest degree of microbial development occurred in the BLA experiment (Fig. 4A) between 7 and 10 days (10,080 and 14,400 min, respectively), similar to what was observed by Puigserver et al. (2016a,b).

In some cases (Fig. 4A), the abundance of bacterial communities in the NAT and COMB experiments decreased. This is what is shown in Fig. 4A, where the height of the colored bar corresponding in the plot to the different experiments decreases because of the number of PCR cycles required to assess the amount of communities would need to be increased (see the Fig. 4 caption). This decline in bacterial communities was caused by the increase in reducing conditions, in which many of the microorganisms cannot survive.

In contrast, in the case of the ZVI experiment (Fig. 4A), a progressive increase in the abundance of microbial communities was observed. This increase is attributable to the fact that the initially high amount of Fe^0 (in the form of mZVI) was toxic to many of the microbial communities (Xue et al., 2018; Daraei et al., 2019). The consumption of the initially introduced mZVI and the adaptation of the microbial communities to the presence of this iron allowed these communities to increase their presence throughout time (Summer et al., 2020; Xu et al., 2021).

The narG gene (nitrate reductase, Table 1 in the SM document) was detected from the start of the experiments. This is consistent with the presence of nitrite in the water sampled at the beginning of the experiments, proving that microorganisms capable of performing the denitrification process naturally exist in the medium (Zielińska et al., 2016; K. Zhang et al., 2019), which further demonstrates that this process takes place at the site.

According to what was observed with the evolution of the concentrations of the nitrogenous compounds (see Section 4.1), a significant increase in the communities encoding the narG gene was observed in the NAT experiment (Fig. 4B) and, to a lesser extent, in the COMB experiment (with the exception of the time of 7 days, 10,080 min, Fig. 4B). By contrast and in accordance with what was observed in the evolution of the concentrations of the nitrogen compounds (see Section 4.1), although a slight increase in the communities encoding this gene was observed in the BLA experiment, after the start of the experiments, the presence of these communities did not show significant differences in general. This, together with the increase in abundance recorded with the 16S (1055f-1392r) primers, demonstrate

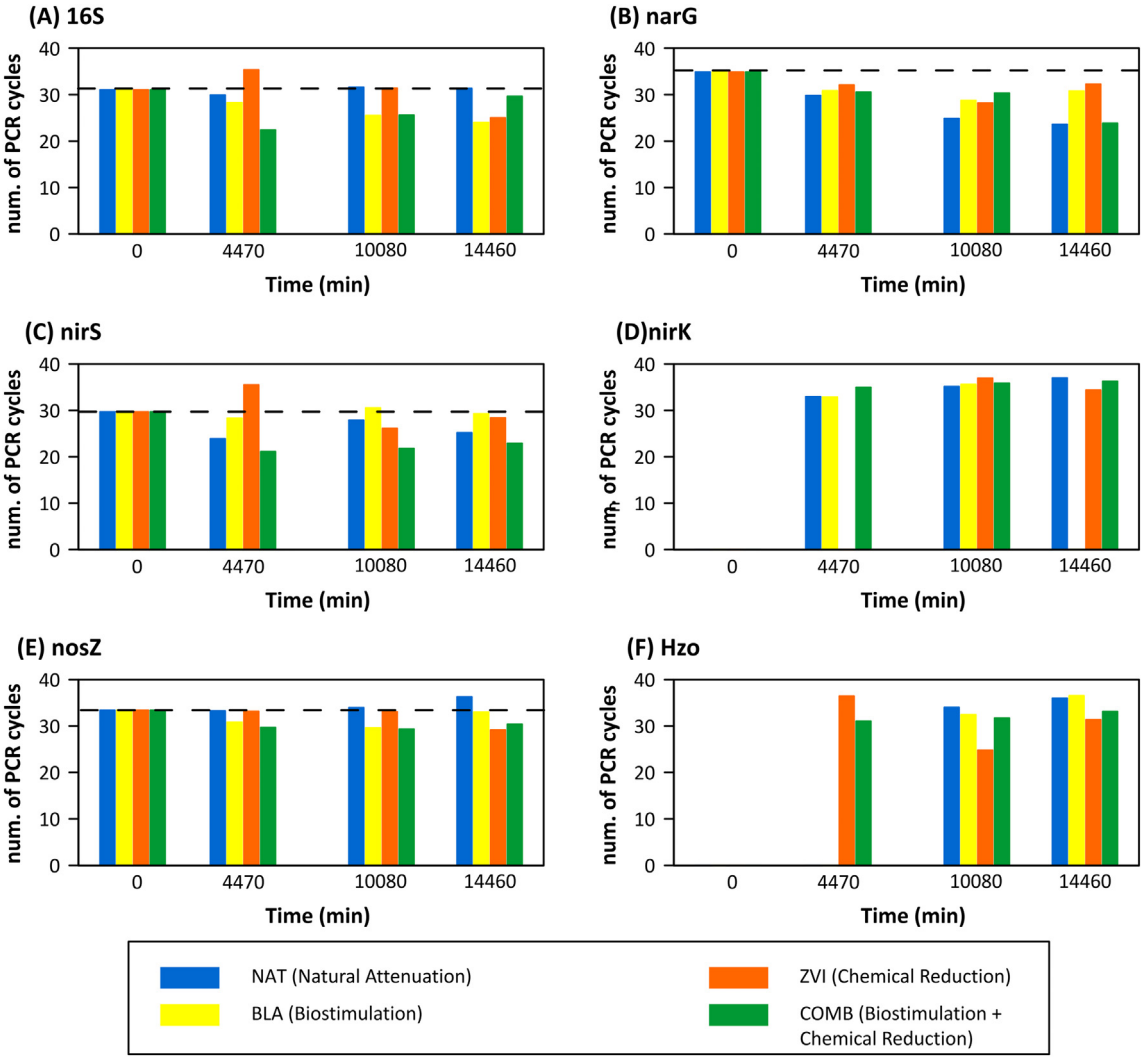

Fig. 4. Temporal evolution of the number of PCR cycles (in semiquantitative units) obtained with the primer 16S (1055f-1392r) reaching the threshold value (Ct) in the treatment test. The relative number of microbial communities present is inversely proportional to the number of PCR cycles required to assess the amount of communities (see Section 3.3.2 and also Section 4 of the SM document regarding the interpretation of Fig. 4). The results obtained with the following genes should be interpreted in a similar way: narg (B), nirS (C), nirS (D), nosZ (E) and Hzo (F).

that biostimulation alone is not a strategy that particularly favors the passage of nitrate to nitrite by denitrification (Garousin et al., 2021).

The reduction of nitrite to NO identified with the nirS gene (nitrite reductase, Table 1 in the SM document) was detected from time 0, which is new evidence that the denitrification process occurs naturally (Zhou et al., 2016; Li et al., 2019; H. Zhang et al., 2019). This contrasts with the absence at time 0 of the nirS gene (nitrite reductase, Table 1 in the SM document, Fig. 4D).

Among all the experiments conducted, the COMB experiment was the one with the highest abundance of the nirS gene (Fig. 4C); although, it decreased slightly throughout the experiment, which confirms that throughout the experiment the denitrification process was at a more advanced stage, favoring the total mineralization of nitrate (Espenberg et al., 2018). This pattern was similar to that observed in the NAT experiment; although, in the latter there was a certain recovery of the presence of this gene at the end (Fig. 4C).

The nirS gene was not detected at the beginning of the experiments. Its presence was observed in the NAT, BLA, and COMB experiments, especially after 3 days (4320 min), decreasing slightly throughout the test (Fig. 4D). This suggests that the denitrifying communities change throughout the experiment, similar to what was observed by Feng et al. (2019). The analysis of this gene shows that the passage of nitrite to NO is frequent in the NAT and COMB scenarios. In contrast, this passage was only observed after 10,080 min (7 days) in the ZVI experiment, which agrees with the toxicity effect of mZVI on bacterial communities. The reduction of NO to NO_2 was not identified as the cnorB gene was practically not observed. However, the presence of the nosZ gene (nitrous oxide reductase) was observed (Fig. 4E), which is in accordance with the observations of Zhang et al. (2021). The progressive increase in this gene in the COMB experiment and its decrease at the end of the NAT experiment is noteworthy (reduction process of NO_2 to N_2 gas). The detection of the nosZ gene from the beginning of the experiments agrees with complete denitrification, even under natural attenuation conditions (Hallin et al., 2018); although, Fig. 4E suggests that the reducing conditions at the end of the experiments favored the increase in this gene in the COMB experiment and its decrease in the NAT, BLA, and ZVI experiments (Song et al., 2015; Wang et al., 2020; Yuan et al., 2021).

The presence of the nirS gene from the beginning of the experiment, the present of the nirS gene after 3 days (4320 min), and the increase in the abundance of this gene in the COMB experiment (Fig. 3C), accompanied by the decrease in ammonium (Fig. 2G, COMB), originated from the abiotic degradation of nitrate by mZVI, suggesting the existence of anaerobic

ammonium oxidation processes such as anammox (Shu et al., 2016; Wang et al., 2019; Podder et al., 2020) in the COMB strategy.

Although the HzsA (hydrazine synthase) and HzsB (hydrazine synthase) genes were analyzed (Table 1 in the SM document), they were not sufficiently detected throughout the experiments, which does not allow for determination of whether N_2H_4 synthesis from NO and ammonium occurred. By contrast, the presence of the Hzo gene (hydrazine oxidoreductase) was detected in some of the samples from a time of 3 days (4320 min) (Fig. 4F). Among the different experiments, the presence of this gene stands out in the ZVI experiment (where an increase in its presence was observed especially at the 7 days) (10,080 min, Fig. 4F). It was also observed that in the COMB experiment this gene (which is related to the occurrence of the anammox reaction, see Section 4 in the SM document) remained constant, which confirms that this reaction occurred very early in the experiment, probably from the beginning, while in the ZVI experiment it occurred significantly late (i.e., at 7 days, 10,080 min), coinciding with the substantial decrease in ammonium concentrations (Fig. 2E, ZVI), similar to what was observed by Wang et al. (2019) and Connan et al. (2016).

4.4. Evolution of chemical and biochemical processes

The processes identified throughout the treatability test were mainly denitrification, Mn and Fe reduction, sulfate reduction, and anammox.

In the case of denitrification, it was observed that this process occurred completely in all the microcosm experiments, but it was in the COMB experiment that it was most effective and with a greater presence of the nosZ gene, which is indicative of the passage from NO to NO_2.

In the case of Mn- and Fe-reduction processes, they were detected in all the experiments, while sulfate reduction was only significantly detected in the COMB experiment and, to a lesser extent, in the ZVI experiment.

Although the anammox process could potentially have occurred in the NAT experiment (as indicated by the presence of enzymes such as those expressed by the Hzo gene), the low ammonium concentrations in the waters sampled at the beginning of the experiment did not make it possible for the process to occur in the NAT and BLA experiments. By contrast, anammox occurred in the ZVI and COMB experiments, where ammonium was produced as a consequence of abiotic nitrate degradation, which generated toxicity problems in the water. Mobilization of ammonium occurred in the COMB experiment because of the more extreme reducing conditions created and the biostimulation of the microbial communities, which gave rise to the anammox process.

4.5. Comparative analysis of the efficiency of the different remediation strategies tested for decreasing nitrate concentrations

Table 3 shows how the most efficient strategy in removing 80 % of the original nitrate (representing a nitrate concentration below the parametric value of 50 mg/L, European Union Directive, 2020) was ZVI, followed by COMB. However, the high production of ammonium generated in the ZVI experiments should be recalled. This cation is toxic (see Sections 1 and 4.1.4). Hence, it is considered that the most efficient strategy is that which, in addition to removing nitrate, is also capable of eliminating the toxic ammonium, which is achieved with the COMB strategy (Table 3). However, the high efficiency of the combined remediation strategy requires appropriate dimensioning of the reagents to be added according to the characteristics of the site. An excess of reagents, and especially of lactic acid for biostimulation, can lead to extremely reducing conditions in the medium. Under these conditions, overgrowth of other microorganisms that do not result in denitrification can occur, and even bioclogging of aquifer effective porosity, or the mobilization of metal ions such as Fe^{2+} and Mn^{2+} from iron or manganese oxide minerals. These ions, under some specific circumstances, can re-precipitate. For example, this can occur with Fe^{2+} (including that from the oxidation of mZVI) if redox conditions favor it. Neoformation pyrite can precipitate if there is dissolved sulfate in the medium and the redox conditions are sulfate-reducing. This can result in a loss of effective porosity and hydraulic conductivity, as in the case of bioclogging. As a consequence, the preferential flow paths may change, so that there may be areas that are no longer accessible to the reagents and therefore untreated. It would therefore be recommendable that, in a second phase, a pilot test be conducted in the field to address these and other key possible issues arising from implementing the COMB strategy in the real world (more information can be found in the SM document).

Table 3
Percentages of efficiency in the mobilization of the original nitrate throughout the microcosm experiments.

Time		Degradation efficiency (% of initial nitrate removed)			
Minutes	Days	NAT	BLA	ZVI	COMB
0	0	0.00	0.00	0.00	0.00
1440	1	29.51	32.34	47.52	53.59
2880	2	59.48	44.73	85.18	79.97
4320	3	81.76	58.62	92.73	91.22
10,080	7	91.59	82.07	96.52	94.16
14,400	10	94.68	96.34	97.29	96.21

5. Conclusions

The use of mZVI for the abiotic degradation of nitrate promotes the formation of ammonium (an undesirable compound due to its high toxicity). By contrast, the strategy resulting from the combination of the use of mZVI coupled with biostimulation of the microbial flora present in the medium causes the anammox process to degrade the harmful ammonium.

The integrated analysis of chemical, isotopic, and biological data shows that the combined strategy favors the denitrification process and results in total mineralization of the original nitrate, which is accompanied by good microbial development of the microorganisms performing this reaction.

The treatability test with microcosm experiments on a laboratory scale shows that the in situ remediation strategy combining ISCR using mZVI and biostimulation with the addition of lactic acid (lactate acting as an electron donor) is a viable strategy for the creation of a reactive zone around supply wells located in regions where groundwater is affected by diffuse nitrate contamination.

The high efficiency of the combined strategy requires an adequate dimensioning of reagents according to the characteristics of the site, since an excess, especially lactic acid, can lead to extremely reducing conditions in the environment. This could favor overgrowth of non-denitrifying bacterial communities, bioclogging of the porosity, mobilization of metal ions such as Fe^{2+} and Mn^{2+}, and even precipitation of neoformation minerals, such as pyrite that (as in bioclogging) can result in a loss of effective porosity and hydraulic conductivity. As a result, preferential flow paths may change, leading to zones that may become inaccessible to the reagents and remain untreated. For this reason, it would be advisable to conduct a pilot study in the field to evaluate how to deal with the problems that may arise during the implementation of the COMB strategy.

CRediT authorship contribution statement

Diana Puigserver: She designed the treatability test, executed and testified the research boreholes. She collected the groundwater and sediments needed for the test at those boreholes. She also sampled the waters in the anaerobic chamber in which the test was carried out and performed the analyses of nitrogen species and other sensitive redox species. She also processed the data, participated in the discussion meetings of the results obtained with the other two authors, and wrote the article.

Jofre Herrero: He performed the enzyme detection analyses and the different molecular techniques necessary for this purpose in the waters sampled during the test. He also carried out the determination of the nitrogen isotopic fractionation of nitrates in these waters to verify that denitrification was occurring. He also carried out the corresponding processing of the data obtained in the enzyme determination and isotopic fractionation. He participated in the discussion meetings of the results obtained together with the other two authors.

José M. Carmona: He participated in the execution of the research drilling boreholes, in the testification, and in their equipment as piezometers. He also supervised the progress of the research and participated in the meetings to discuss the results obtained with the other two authors.

Declaration of competing interest

The authors of this research paper (Diana Puigserver, Jofre Herrero and José M. Carmona) declare that they have no known competing financial interests or personal relationships that could have appeared to influence the work reported in this paper.

Acknowledgments

We would like to thank the Catalan Water Agency and the Bosch i Gimpera Foundation for funding this research (project code: FBG-310769).

Appendix A. Supplementary data

Supplementary data to this article can be found online at https://doi.org/10.1016/j.scitotenv.2022.156841.

References

Abiriga, D., Vestgarden, L.S., Klempe, H., 2021. Long-term redox conditions in a landfill-leachate-contaminated groundwater. Sci. Total Environ. 755, 143725.
Aravena, R., Robertson, W.D., 1998. Use of multiple isotope tracers to evaluate denitrification in ground water: study of nitrate from a large-flux septic system plume. Groundwater 36 (6), 975–982.
Ascott, M.J., Wang, L., Stuart, M.E., Ward, R.S., Hart, A., 2016. Quantification of nitrate storage in the vadose (unsaturated) zone: a missing component of terrestrial N budgets. Hydrol. Process. 30 (12), 1903–1915.
Ashok, V., Hait, S., 2015. Remediation of nitrate-contaminated water by solid-phase denitrification process—a review. Environ. Sci. Pollut. Res. 22 (11), 8075–8093.
Bertrand, J.C., Doumenq, P., Guyoneaud, R., Marrot, B., Martin-Laurent, F., Matheron, R., Soulas, G., 2015. Applied microbial ecology and bioremediation. Environmental Microbiology: Fundamentals and Applications. Springer, Dordrecht, pp. 659–753.
Bhateria, R., Jain, D., 2016. Water quality assessment of lake water: a review. Sustain. Water Resour. Manag. 2 (2), 161–173.
Biddau, R., Cidu, R., Da Pelo, S., Carletti, A., Ghiglieri, G., Pittalis, D., 2019. Source and fate of nitrate in contaminated groundwater systems: assessing spatial and temporal variations by hydrogeochemistry and multiple stable isotope tools. Sci. Total Environ. 647, 1121–1136.
Braker, G., Zhou, J., Wu, L., Devol, A.H., Tiedje, J.M., 2000. Nitrite reductase genes (nirS and nirK) as functional markers to investigate diversity of denitrifying bacteria in Pacific northwest marine sediment communities. Appl. Environ. Microbiol. 66 (5), 2096–2104.
Canter, L.W., 2019. Management measures for nitrate pollution prevention. Nitrates in Groundwater. Routledge, pp. 183–216.
Capodaglio, A.G., Hlavínek, P., Raboni, M., 2016. Advances in wastewater nitrogen removal by biological processes: state of the art review. Revista Ambiente Agua 11, 250–267.
Caschetto, M., 2017. Ammonium natural attenuation in complex hydrogeological settings: insights from a multi-isotope approach. Acque SotterraneeItal. J. Groundw. 6 (4).
Chang, N.B., Imen, S., Vannah, B., 2015. Remote sensing for monitoring surface water quality status and ecosystem state in relation to the nutrient cycle: a 40-year perspective. Crit. Rev. Environ. Sci. Technol. 45 (2), 101–166.
Chen, Y.M., Li, C.W., Chen, S.S., 2005. Fluidized zero valent iron bed reactor for nitrate removal. Chemosphere 59 (6), 753–759.
Chen, Y.P., Li, S., Ning, Y.F., Hu, N.N., Cao, H.H., Fang, F., Guo, J.S., 2012. Start-up of completely autotrophic nitrogen removal over nitrite enhanced by hydrophilic-modified carbon fiber. Appl. Biochem. Biotechnol. 166 (4), 866–877.
Christensen, T.H., Bjerg, P.L., Banwart, S.A., Jakobsen, R., Heron, G., Albrechtsen, H.J., 2000. Characterization of redox conditions in groundwater contaminant plumes. J. Contam. Hydrol. 45 (3–4), 165–241.
Connan, R., Dabert, P., Khalil, H., Bridoux, G., Béline, F., Magrí, A., 2016. Batch enrichment of anammox bacteria and study of the underlying microbial community dynamics. Chem. Eng. J. 297, 217–228.
Cullen, L.G., Tilston, E.L., Mitchell, G.R., Collins, C.D., Shaw, L.J., 2011. Assessing the impact of nano-and micro-scale zerovalent iron particles on soil microbial activities: particle reactivity interferes with assay conditions and interpretation of genuine microbial effects. Chemosphere 82 (11), 1675–1682.
Daraei, H., Rafiee, M., Yazdanbakhsh, A.R., Amoozegar, M.A., Guanglei, Q., 2019. A comparative study on the toxicity of nano zero valent iron (nZVI) on aerobic granular sludge and flocculent activated sludge: reactor performance, microbial behavior, and mechanism of toxicity. Process Saf. Environ. Prot. 129, 238–248.
Della Rocca, C., Belgiorno, V., Meriç, S., 2007. Overview of in-situ applicable nitrate removal processes. Desalination 204 (1–3), 46–62.
Demeke, A., Tassew, A., 2016. A review on water quality and its impact on fish health. Int. J. Fauna Biol. Stud. 3 (1), 21–31.
Di Lorenzo, T., Cifoni, M., Lombardo, P., Fiasca, B., Galassi, D.M.P., 2015. Ammonium threshold values for groundwater quality in the EU may not protect groundwater fauna: evidence from an alluvial aquifer in Italy. Hydrobiologia 743 (1), 139–150.
Di Lorenzo, T., Fiasca, B., Di Cicco, M., Galassi, D.M.P., 2021. The impact of nitrate on the groundwater assemblages of european unconsolidated aquifers is likely less severe than expected. Environ. Sci. Pollut. Res. 28 (9), 11518–11527.
Dubrovsky, N.M., Hamilton, P.A., 2010. The quality of our nation's water: nutrients in the nation's streams and groundwater; national findings and implications. US Geological Survey, National Water-Quality Assessment Program, pp. 2010–3078.
Espenberg, M., Truu, M., Mander, Ü., Kasak, K., Nõlvak, H., Ligi, T., Truu, J., 2018. Differences in microbial community structure and nitrogen cycling in natural and draineer d tropical peatland soils. Sci. Rep. 8 (1), 1–12.
European Union Directive, 2020. Directive (EU) 2020/2184 of the European Parliament and of the Council of 16 December 2020 on the Quality of Water Intended for Human Consumption (Recast).
Feng, L., Pi, S., Zhu, W., Wang, X., Xu, X., 2019. Nitrification and aerobic denitrification in solid phase denitrification systems with various biodegradable carriers for ammonium-contaminated water purification. J. Chem. Technol. Biotechnol. 94 (11), 3569–3577.
Garousin, H., Pourbabaee, A.A., Alikhani, H.A., Yazdanfar, N., 2021. A combinational strategy mitigated old-aged petroleum contaminants: ineffectiveness of biostimulation as a bioremediation technique. Front. Microbiol. 12, 363.
Ghane, E., Fausey, N.R., Brown, L.C., 2015. Modeling nitrate removal in a denitrification bed. Water Res. 71, 294–305.
Grau-Martínez, A., Torrentó, C., Carrey, R., Soler, A., Otero, N., 2019. Isotopic evidence of nitrate degradation by a zero-valent iron permeable reactive barrier: batch experiments and a field scale study. J. Hydrol. 570, 69–79.
Guo, J., Zuo, P., Yang, L., Pan, Y., Wang, L., 2021. Quantitative identification of non-point sources of nitrate in urban canals based on dense in-situ samplings and nitrate isotope composition. Chemosphere 263, 128219.
Hallin, S., Philippot, L., Löffler, F.E., Sanford, R.A., Jones, C.M., 2018. Genomics and ecology of novel N2O-reducing microorganisms. Trends Microbiol. 26 (1), 43–55.
Hansen, B., Sonnenborg, T.O., Møller, I., Bernth, J.D., Høyer, A.S., Rasmussen, P., Jørgensen, F., 2016. Nitrate vulnerability assessment of aquifers. Environ. Earth Sci. 75 (12), 1–15.
Herrero, J., Puigserver, D., Nijenhuis, I., Kuntze, K., Carmona, J.M., 2019. Combined use of ISCR and biostimulation techniques in incomplete processes of reductive dehalogenation of chlorinated solvents. Sci. Total Environ. 648, 819–829.
Hinshaw, S.E., Zhang, T., Harrison, J.A., Dahlgren, R.A., 2020. Excess N2 and denitrification in hyporheic porewaters and groundwaters of the San Joaquin River, California. Water Res. 168, 115161.
Huang, S., Chen, C., Yang, X., Wu, Q., Zhang, R., 2011. Distribution of typical denitrifying functional genes and diversity of the nirS-encoding bacterial community related to environmental characteristics of river sediments. Biogeosciences 8 (10), 3041–3051.
Istok, J.D., Park, M.M., Peacock, A.D., Oostrom, M., Wietsma, T.W., 2007. An experimental investigation of nitrogen gas produced during denitrification. Groundwater 45 (4), 461–467.
Jahangir, M.M., Khalil, M.I., Johnston, P., Cardenas, L.M., Hatch, D.J., Butler, M., Richards, K.G., 2012. Denitrification potential in subsoils: a mechanism to reduce nitrate leaching to groundwater. Agric. Ecosyst. Environ. 147, 13–23.
Jetten, M.S., Wagner, M., Fuerst, J., van Loosdrecht, M., Kuenen, G., Strous, M., 2001. Microbiology and application of the anaerobic ammonium oxidation ('anammox') process. Curr. Opin. Biotechnol. 12 (3), 283–288.
Jia, T., Wang, Z., Shan, H., Liu, Y., Gong, L., 2017. Effect of nanoscale zero-valent iron on sludge anaerobic digestion. Resour. Conserv. Recycl. 127, 190–195.
Jørgensen, P.R., Urup, J., Helstrup, T., Jensen, M.B., Eiland, F., Vinther, F.P., 2004. Transport and reduction of nitrate in clayey till underneath forest and arable land. J. Contam. Hydrol. 73 (1–4), 207–226.
Karimian, N., Johnston, S.G., Burton, E.D., 2018. Iron and sulfur cycling in acid sulfate soil wetlands under dynamic redox conditions: a review. Chemosphere 197, 803–816.
Karunanidhi, D., Aravinthasamy, P., Subramani, T., Kumar, D., Setia, R., 2021. Investigation of health risks related with multipath entry of groundwater nitrate using sobol sensitivity indicators in an urban-industrial sector of South India. Environ. Res. 200, 111726.
Kaur, L., Rishi, M.S., Siddiqui, A.U., 2020. Deterministic and probabilistic health risk assessment techniques to evaluate non-carcinogenic human health risk (NHHR) due to fluoride and nitrate in groundwater of Panipat, Haryana, India. Environ. Pollut. 259, 113711.
Keiner, R., Herrmann, M., Küsel, K., Popp, J., Frosch, T., 2015. Rapid monitoring of intermediate states and mass balance of nitrogen during denitrification by means of cavity enhanced Raman multi-gas sensing. Anal. Chim. Acta 864, 39–47.
Kim, K.H., Yun, S.T., Kim, H.K., Kim, J.W., 2015. Determination of natural backgrounds and thresholds of nitrate in south korean groundwater using model-based statistical approaches. J. Geochem. Explor. 148, 196–205.
Klement, L., Bach, M., Breuer, L., Häußermann, U., 2017. Groundwater nitrate pollution: High-resolution approach of calculating the nitrogen balance surplus for Germany. *EGU General Assembly Conference Abstracts*. European Geosciences Union, p. 15032.
Koppria, G.A., Kattner, G., Freije, R.H., de Paggi, S.J., Lara, R.J., 2014. Seasonal baseline of nutrients and stable isotopes in a saline lake of Argentina: biogeochemical processes and river runoff effects. Environ. Monit. Assess. 186 (5), 3139–3148.
Langone, M., Yan, J., Haaijer, S.C.M., Op den Camp, H.J., Jetten, M., Andreottola, G., 2014. Coexistence of nitrifying, anammox and denitrifying bacteria in a sequencing batch reactor. Front. Microbiol. 5, 28.
Lasagna, M., De Luca, D.A., Franchino, E., 2016. Nitrate contamination of groundwater in the western Po plain (Italy): the effects of groundwater and surface water interactions. Environ. Earth Sci. 75 (3), 240.
Lee, D., Lee, J., Gil, K., 2021. Determination optimal ratio of ammonium to nitrite in application of the ANAMMOX process in the mainstream. J. Wetlands Res. 23 (1), 60–66.

Levy, Y., Shapira, R.H., Chefetz, B., Kurtzman, D., 2017. Modeling nitrate from land surface to wells' perforations under agricultural land: success, failure, and future scenarios in a Mediterranean case study. Hydrol. Earth Syst. Sci. 21 (7), 3811–3825.
Li, J., Wang, J.T., Hu, H.W., Cai, Z.J., Lei, Y.R., Li, W., Cui, L.J., 2019. Changes of the denitrifying communities in a multi-stage free water surface constructed wetland. Sci. Total Environ. 650, 1419–1425.
Liu, H., Chen, Z., Guan, Y., Xu, S., 2018. Role and application of iron in water treatment for nitrogen removal: a review. Chemosphere 204, 51–62.
Liu, Y., Wang, J., 2019. Reduction of nitrate by zero valent iron (ZVI)-based materials: a review. Sci. Total Environ. 671, 388–403.
Liu, G.D., Wu, W.L., Zhang, J., 2005. Regional differentiation of non-point source pollution of agriculture-derived nitrate nitrogen in groundwater in northern China. Agric. Ecosyst. Environ. 107 (2–3), 211–220.
McLeod, H.C., Roy, J.W., Slater, G.F., Smith, J.E., 2018. Anaerobic biodegradation of dissolved ethanol in a pilot-scale sand aquifer: variability in plume (redox) biogeochemistry. J. Contam. Hydrol. 208, 35–45.
McMahon, P.B., Belitz, K., Reddy, J.E., Johnson, T.D., 2018. Elevated manganese concentrations in United States groundwater, role of land surface–soil–aquifer connections. Environ. Sci. Technol. 53 (1), 29–38.
Merchán, D., Sanz, L., Alfaro, A., Pérez, I., Goñi, M., Solsona, F., Casalí, J., 2020. Irrigation implementation promotes increases in salinity and nitrate concentration in the lower reaches of the Cidacos River (Navarre, Spain). Sci. Total Environ. 706, 135701.
Miao, L., Yang, G., Tao, T., Peng, Y., 2019. Recent advances in nitrogen removal from landfill leachate using biological treatments–A review. J. Environ. Manag. 235, 178–185.
Mohanadhas, B., Kumar, G.S., 2019. Numerical experiments on fate and transport of benzene with biological clogging in vadoze zone. Environmental Processes 6 (4), 841–858.
Molognoni, D., Devecseri, M., Cecconet, D., Capodaglio, A.G., 2017. Cathodic groundwater denitrification with a bioelectrochemical system. Journal of Water Process Engineering 19, 67–73.
Munz, M., Oswald, S.E., Schäfferling, R., Lensing, H.J., 2019. Temperature-dependent redox zonation, nitrate removal and attenuation of organic micropollutants during bank filtration. Water Res. 162, 225–235.
Paerl, H.W., Scott, J.T., McCarthy, M.J., Newell, S.E., Gardner, W.S., Havens, K.E., Wurtsbaugh, W.A., 2016. It takes two to tango: when and where dual nutrient (N & P) reductions are needed to protect lakes and downstream ecosystems. Environ. Sci. Technol. 50 (20), 10805–10813.
Park, G.W., Fei, Q., Jung, K., Chang, H.N., Kim, Y.C., Kim, N.J., Cho, J., 2014. Volatile fatty acids derived from waste organics provide an economical carbon source for microbial lipids/biodiesel production. Biotechnol. J. 9 (12), 1536–1546.
Park, S., Kim, H.K., Kim, M.S., Lee, G.M., Song, D.H., Jeon, S.H., Kim, T.S., 2016. Monitoring nitrate natural attenuation and analysis of indigenous micro-organism community in groundwater. Desalin. Water Treat. 57 (51), 24096–24108.
Pedersen, L.L., Smets, B.F., Dechesne, A., 2015. Measuring biogeochemical heterogeneity at the micro scale in soils and sediments. Soil Biol. Biochem. 90, 122–138.
Peng, L., Liu, Y., Gao, S.H., Chen, X., Ni, B.J., 2016. Evaluating simultaneous chromate and nitrate reduction during microbial denitrification processes. Water Res. 89, 1–8.
Podder, A., Reinhart, D., Goel, R., 2020. Nitrogen management in landfill leachate using single-stage anammox process-illustrating key nitrogen pathways under an ecogenomics framework. Bioresour. Technol. 312, 123578.
Puigserver, D., Carmona, J.M., Cortés, A., Viladevall, M., Nieto, J.M., Grifoll, M., Parker, B.L., 2013. Subsoil heterogeneities controlling porewater contaminant mass and microbial diversity at a site with a complex pollution history. J. Contam. Hydrol. 144 (1), 1–19.
Puigserver, D., Herrero, J., Torres, M., Cortés, A., Nijenhuis, I., Kuntze, K., Carmona, J.M., 2016. Reductive dechlorination in recalcitrant sources of chloroethenes in the transition zone between aquifers and aquitards. Environ. Sci. Pollut. Res. 23 (18), 18724–18741.
Puigserver, D., Nieto, J.M., Grifoll, M., Vila, J., Cortés, A., Viladevall, M., Carmona, J.M., 2016. Temporal hydrochemical and microbial variations in microcosm experiments from sites contaminated with chloromethanes under biostimulation with lactic acid. Bioremediation Journal 20 (1), 54–70.
Qambrani, N.A., Jung, S.H., Ok, Y.S., Kim, Y.S., Oh, S.E., 2013. Nitrate-contaminated groundwater remediation by combined autotrophic and heterotrophic denitrification for sulfate and pH control: batch tests. Environ. Sci. Pollut. Res. 20 (12), 9084–9091.
Qin, S., Yu, L., Yang, Z., Li, M., Clough, T., Wrage-Mönnig, N., Zhou, S., 2019. Electrodes donate electrons for nitrate reduction in a soil matrix via DNRA and denitrification. Environ. Sci. Technol. 53 (4), 2002–2012.
Re, V., Sacchi, E., Kammoun, S., Tringali, C., Trabelsi, R., Zouari, K., Daniele, S., 2017. Integrated socio-hydrogeological approach to tackle nitrate contamination in groundwater resources. The case of Grombalia Basin (Tunisia). Sci. Total Environ. 593, 664–676.
Rivett, M.O., Buss, S.R., Morgan, P., Smith, J.W., Bemment, C.D., 2008. Nitrate attenuation in groundwater: a review of biogeochemical controlling processes. Water Res. 42 (16), 4215–4232.
Rodríguez-Maroto, J.M., García-Herruzo, F., García-Rubio, A., Gómez-Lahoz, C., Vereda-Alonso, C., 2009. Kinetics of the chemical reduction of nitrate by zero-valent iron. Chemosphere 74 (6), 804–809.
Romanelli, A., Soto, D.X., Matiatos, I., Martínez, D.E., Esquius, S., 2020. A biological and nitrate isotopic assessment framework to understand eutrophication in aquatic ecosystems. Sci. Total Environ. 715, 136909.
Ruan, X., Yin, J., Cui, X., Li, N., Shen, D., 2020. Bioaugmentation and quorum sensing disruption as solutions to increase nitrate removal in sequencing batch reactors treating nitrate-rich wastewater. J. Environ. Sci. 98, 179–185.
Schullehner, J., Hansen, B., Thygesen, M., Pedersen, C.B., Sigsgaard, T., 2018. Nitrate in drinking water and colorectal cancer risk: a nationwide population-based chort study. Int. J. Cancer 143 (1), 73–79.
Serio, F., Miglietta, P.P., Lamastra, L., Ficocelli, S., Intini, F., De Leo, F., De Donno, A., 2018. Groundwater nitrate contamination and agricultural land use: a grey water footprint perspective in southern Apulia region (Italy). Sci. Total Environ. 645, 1425–1431.
Sheng, S., Liu, B., Hou, X., Liang, Z., Sun, X., Du, L., Wang, D., 2018. Effects of different carbon sources and C/N ratios on the simultaneous anammox and denitrification process. Int. Biodeterior. Biodegradation 127, 26–34.
Shu, D., He, Y., Yue, H., Yang, S., 2016. Effects of fe (II) on microbial communities, nitrogen transformation pathways and iron cycling in the anammox process: kinetics, quantitative molecular mechanism and metagenomic analysis. RSC Adv. 6 (72), 68005–68016.
Shukla, S., Saxena, A., 2018. Global status of nitrate contamination in groundwater: its occurrence, health impacts, and mitigation measures. Handbook of Environmental Materials Management, pp. 869–888.
Smith, R.L., Bohlke, J.K., Song, B., Tobias, C.R., 2015. Role of anaerobic ammonium oxidation (anammox) in nitrogen removal from a freshwater aquifer. Environmental science & technology 49 (20), 12169–12177.
Song, K., Harper, W.F., Hori, T., Riya, S., Hosomi, M., Terada, A., 2015. Impact of carbon sources on nitrous oxide emission and microbial community structure in an anoxic/oxic activated sludge system. Clean Techn. Environ. Policy 17 (8), 2375–2385.
Su, Z., Zhang, Y., Jia, X., Xiang, X., Zhou, J., 2020. Research on enhancement of zero-valent iron on dissimilatory nitrate/nitrite reduction to ammonium of Desulfovibrio sp. CMX. Sci. Total Environ. 746, 141126.
Summer, D., Schöftner, P., Watzinger, A., Reichenauer, T.G., 2020. Inhibition and stimulation of two perchloroethene degrading bacterial cultures by nano-and micro-scaled zero-valent iron particles. Sci. Total Environ. 722, 137802.
Sunger, N., Bose, P., 2009. Autotrophic denitrification using hydrogen generated from metallic iron corrosion. Bioresour. Technol. 100 (18), 4077–4082.
Temkin, A., Evans, S., Manidis, T., Campbell, C., Naidenko, O.V., 2019. Exposure-based assessment and economic valuation of adverse birth outcomes and cancer risk due to nitrate in United States drinking water. Environ. Res. 176, 108442.
Tiedje, J.M., 1994. Denitrifiers. Methods of Soil Analysis: Part 2 Microbiological and Biochemical Properties. 5, pp. 245–267.
Trevors, J.T., 1996. Sterilization and inhibition of microbial activity in soil. J. Microbiol. Methods 26 (1–2), 53–59.
Trouwborst, R.E., Clement, B.G., Tebo, B.M., Glazer, B.T., Luther, G.W., 2006. Soluble Mn (III) in suboxic zones. Science 313 (5795), 1955–1957.
Vavilin, V.A., Rytov, S.V., 2015. Nitrate denitrification with nitrite or nitrous oxide as intermediate products: stoichiometry, kinetics and dynamics of stable isotope signatures. Chemosphere 134, 417–426.
Wallenstein, M.D., Myrold, D.D., Firestone, M., Voytek, M., 2006. Environmental controls on denitrifying communities and denitrification rates: insights from molecular methods. Ecol. Appl. 16 (6), 2143–2152.
Wang, Q.H., Yu, L.J., Liu, Y., Lin, L., Lu, R.G., Zhu, J.P., Lu, Z.L., 2017. Methods for the detection and determination of nitrite and nitrate: a review. Talanta 165, 709–720.
Wang, D., He, Y., Zhang, X.X., 2019. A comprehensive insight into the functional bacteria and genes and their roles in simultaneous denitrification and anammox system at varying substrate loadings. Appl. Microbiol. Biotechnol. 103 (3), 1523–1533.
Wang, L., Zhou, Y., Peng, F., Zhang, A., Pang, Q., Lian, J., Cui, Y., 2020. Intensified nitrogen removal in the tidal flow constructed wetland-microbial fuel cell: insight into evaluation of denitrifying genes. J. Clean. Prod. 264, 121580.
Ward, M.H., Jones, R.R., Brender, J.D., De Kok, T.M., Weyer, P.J., Nolan, B.T., Van Breda, S.G., 2018. Drinking water nitrate and human health: an updated review. Int. J. Environ. Res. Public Health 15 (7), 1557.
Wells, N.S., Clough, T.J., Johnson-Beebout, S.E., Elberling, B., Baisden, W.T., 2019. Effects of denitrification and transport on the isotopic composition of nitrate (δ18O, δ15N) in freshwater systems. Sci. Total Environ. 651, 2228–2234.
Wenk, C.B., Zopfi, J., Blees, J., Veronesi, M., Niemann, H., Lehmann, M.F., 2014. Community N and O isotope fractionation by sulfide-dependent denitrification and anammox in a stratified lacustrine water column. Geochim. Cosmochim. Acta 125, 551–563.
Wongsanit, J., Teartisup, P., Kerdsueb, P., Tharnpoophasiam, P., Worakhunpiset, S., 2015. Contamination of nitrate in groundwater and its potential human health: a case study of lower Mae Klong river basin, Thailand. Environ. Sci. Pollut. Res. 22 (15), 11504–11512.
Xie, Y., Dong, H., Zeng, G., Tang, L., Jiang, Z., Zhang, C., Zhang, Y., 2017. The interactions between nanoscale zero-valent iron and microbes in the subsurface environment: a review. J. Hazard. Mater. 321, 390–407.
Xu, Y., Tang, Y., Xu, L., Wang, Y., Liu, Z., Qin, Q., 2021. Effects of iron-carbon materials on microbial-catalyzed reductive dechlorination of polychlorinated biphenyls in taihu Lake sediment microcosms: enhanced chlorine removal, detoxification and shifts of microbial community. Sci. Total Environ. 148454.
Xue, D., De Baets, B., Van Cleemput, O., Hennessy, C., Berglund, M., Boeckx, P., 2012. Use of a bayesian isotope mixing model to estimate proportional contributions of multiple nitrate sources in surface water. Environ. Pollut. 161, 43–49.
Xue, W., Huang, D., Zeng, G., Wan, J., Cheng, M., Zhang, C., Li, J., 2018. Performance and toxicity assessment of nanoscale zero valent iron particles in the remediation of contaminated soil: a review. Chemosphere 210, 1145–1156.
Yang, Y., Yang, F., Huang, W., Huang, W., Li, F., Lei, Z., Zhang, Z., 2018. Enhanced anaerobic digestion of ammonia-rich swine manure by zero-valent iron: with special focus on the enhancement effect on hydrogenotrophic methanogenesis activity. Bioresour. Technol. 270, 172–179.
Yuan, H., Huang, S., Yuan, J., You, Y., Zhang, Y., 2021. Characteristics of microbial denitrification under different aeration intensities: per et formance, mechanism, and co-occurrence network. Sci. Total Environ. 754, 141965.
Zhang, Y., Li, F., Zhang, Q., Li, J., Liu, Q., 2014. Tracing nitrate pollution sources and transformation in surface-and ground-waters using environmental isotopes. Sci. Total Environ. 490, 213–222.
Zhang, W., Ruan, X., Bai, Y., Yin, L., 2018. The characteristics and performance of sustainable-releasing compound carbon source material applied on groundwater nitrate in-situ remediation. Chemosphere 205, 635–642.

Zhang, H., Feng, J., Chen, S., Zhao, Z., Li, B., Wang, Y., Hao, H., 2019. Geographical patterns of nirS gene abundance and nirS-type denitrifying bacterial community associated with activated sludge from different wastewater treatment plants. Microb. Ecol. 77 (2), 304–316.

Zhang, K., Gu, J., Wang, X., Zhang, X., Hu, T., Zhao, W., 2019. Analysis for microbial denitrification and antibiotic resistance during anaerobic digestion of cattle manure containing antibiotic. Bioresour. Technol. 291, 121803.

Zhang, Y., Douglas, G.B., Kaksonen, A.H., Cui, L., Ye, Z., 2019. Microbial reduction of nitrate in the presence of zero-valent iron. Sci. Total Environ. 646, 1195–1203.

Zhang, W., Niu, W., Li, G., Wang, J., Wang, Y., Dong, A., 2020. Lateral inner environment changes and effects on emitter clogging risk for different irrigation times. Agric. Water Manag. 233, 106069.

Zhang, X., Wu, P., Ma, L., Chen, J., Wang, C., Liu, W., Xu, L., 2021. A novel simultaneous partial nitrification and denitratation (SPND) process in single micro-aerobic sequencing batch reactor for stable nitrite accumulation under ambient temperature. Chem. Eng. J. 130646.

Zhong, X., Wu, Y., 2013. Bioclogging in porous media under continuous-flow condition. Environ. Earth Sci. 68 (8), 2417–2425.

Zhou, S., Huang, T., Zhang, C., Fang, K., Xia, C., Bai, S., Qiu, X., 2016. Illumina MiSeq sequencing reveals the community composition of NirS-type and NirK-type denitrifiers in zhoucun reservoir–a large shallow eutrophic reservoir in northern China. RSC Adv. 6 (94), 91517–91528.

Zhou, Z., Chen, J., Meng, H., et al., 2017. New PCR primers targeting hydrazine synthase and cytochrome c biogenesis proteins in anammox bacteria. Appl. Microbiol. Biotechnol. 101, 1267–1287. https://doi.org/10.1007/s00253-016-8013-7.

Zielińska, M., Rusanowska, P., Jarząbek, J., Nielsen, J.L., 2016. Community dynamics of denitrifying bacteria in full-scale wastewater treatment plants. Environ. Technol. 37 (18), 2358–2367.